Steel and Composite Structures, *Vol. 19, No. 4 (2015) 861-876*
DOI: http://dx.doi.org/10.12989/scs.2015.19.4.861

Elastic-plastic formulation for concrete encased sections interaction diagram tracing

Ernesto Fenollosa [*1], Enrique Gil [1], Ivan Cabrera [1] and Jose Vercher [2]

[1] *Department of Continuum Mechanics and Theory of Structures, Polytechnic University of Valencia, Cno. de Vera s/n 46022 Valencia, Spain*
[2] *Department of Architectural Constructions, Polytechnic University of Valencia, Cno. de Vera s/n 46022 Valencia, Spain*

(*Received April 16, 2014, Revised January 23, 2015, Accepted March 03, 2015*)

Abstract. Composite sections design consists on checking that the point defined by axial load and bending moment keeps included within the surface enclosed by the section interaction curve. Eurocode 4 suggests a method for tracing this diagram based on the plastic stress distribution method. However curves obtained according to this criterion overvalue concrete encased sections bearing capacity, especially when axial force comes with high bending moment values, so a correction factor is required. This article proposes a method for tracing this diagram based on the strain compatibility method. When stresses on the section are integrated by considering the Navier hypothesis, the use of the materials nonlinear constitutive equations provides curves much more adjusted to reality. This process requires the use of rather complex software which might reveal as too complex for practitioners. Preserving the same criteria of an elastic-plastic stress distribution, this article presents alternative expressions to obtain the failure internal forces in five significant points of the interaction diagram having considered five different positions of the neutral axis. These expressions are simply enough for their practical application. Concordance of curves traced strictly relying on these five points with those obtained by computer assisted stress integration considering the strain compatibility method and even with Eurocode 4 weighted curves will be presented for three different cross-sections and two different concrete strengths, revealing very good results.

Keywords: concrete encased sections; interaction diagrams; Eurocode 4; plastic; elastic-plastic

1. Introduction

Composite columns are structural elements formed by reinforced concrete and a steel profile, usually under mainly axial compression but it may appear accompanied by one or two bending moments. These materials which they are composed of endow them with a big strength for high loads with relatively small sections (Griffis *et al*. 2003). That makes them specially appropriated for high-rise buildings.

The most usual composite columns in building are the concrete-encased structural steel and the concrete filled tubes. First ones present not only good strength but also a good behavior both about

∗Corresponding author, Ph.D., E-mail: efenollo@mes.upv.es

http://www.techno-press.org/?journal=scs&subpage=8 ISSN: 1229-9367 (Print), 1598-6233 (Online)

corrosion and with fire. Many times it is required to turn to this typology for reaching the fire stability times required by current laws (Johnson 2004).

Because of its increasing use since mid-twentieth century, researchers have carried out abundant tests (Shanmugam and Lakshmi 2001, Tokgoz and Dundar 2008, Soliman *et al*. 2013) and have suggested numerous design methods. Most of the national codes which inspired the current laws come from these investigations. The most standing-out among them are Load and Resistance Factor Design (AISC 2005), the British BS5400 (2005) and Eurocode 4 (EC4 2011).

The comparative study of the above mentioned codes (Saw and Richard Liew 2000) shows that EC4 endows short columns with a higher bearing capacity. Furthermore it indicates that for axially loaded columns obtained values are acceptable and those for eccentrically loaded columns these results are too tight. The representation of failure load values for several columns tested in laboratory on interaction diagrams traced according to Eurocode 4 (Ellobody *et al*. 2011) show clearly that its method is extremely tight.

ABAQUS enables us to model several columns with finite elements and to develop a non-linear process. Failure load analysis done by means of this software (Ellobody and Young 2011) reveals that Eurocode 4 predicts properly the axial force value but overestimates the bending moment value.

Tracing correctly the cross-section interaction diagram is extremely important for composite columns design (Jung *et al*. 2005). Thus this article undertakes the task of comparing both procedures for its tracing: the plastic stress distribution method used by Eurocode 4 and the strain compatibility method used by the authors.

When comparing both obtained interaction diagrams it can be observed that first one endows the concrete encased sections a higher bearing capacity when the axial force appears accompanied by high bending moments. Up to an 8%, this difference means that applying Eurocode 4 method might overvalue slender columns strength under strong seismic forces if the α_M coefficient weren't considered.

The strain compatibility method provides more precise results with no need of weighting when bending moment values prevail. However, the P-M diagram tracing under this hypothesis is rather more complex as long as stresses are not constant all over the section and integration is required.

In order to avoid this complexity, but preserving the consideration of an elastic-plastic behavior for materials, this research will present a formulation concordant enough with a pure computer assisted strain compatibility method application and simple enough so as to be used in technical offices.

2. Composite section interaction diagram

The EC4 method is based on the work of Roik and Bergmann (1989) and relies on the cross-section interaction diagram. Its field of application is restricted to sections with double symmetry, with no changes along the whole bar length and with a relative slenderness not higher than 2. But these conditions are rather usual in building structures.

According to the above mentioned code, four significant points of the interaction diagram can be determined accepting rectangular stresses distribution (plastic stress distribution method) by applying the equilibrium conditions for forces and moments.

Fig. 1(a) depicts an interaction diagram for a typical concrete encased section displaying its representative points with the hereunder failure forces.

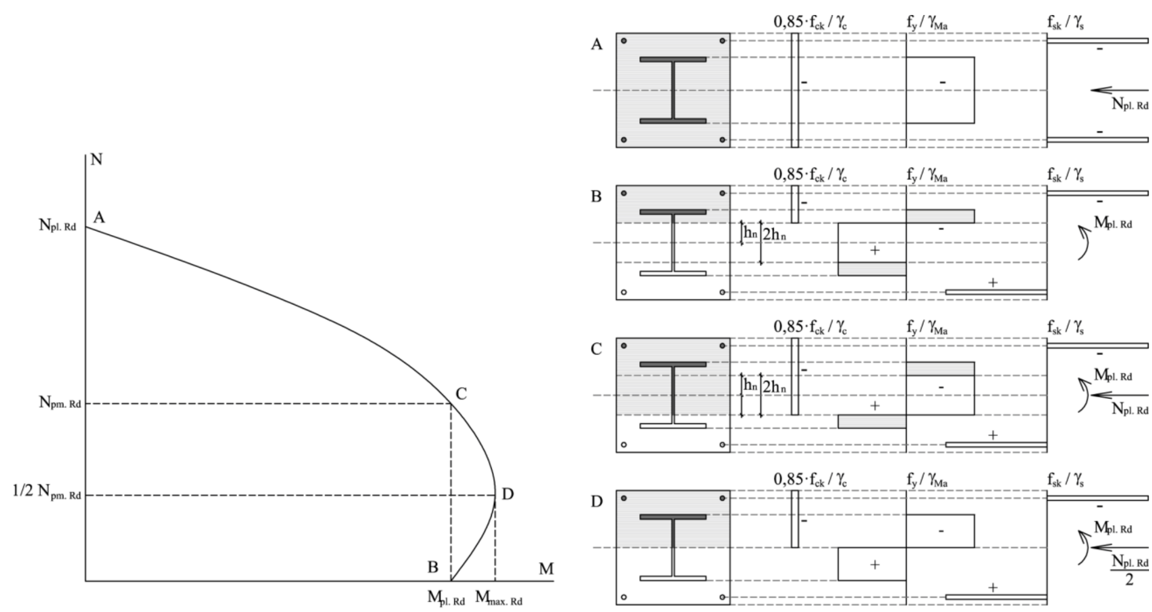

(a) Section interaction diagram (b) Stresses blocks

Fig. 1 Interaction diagram according to Eurocode 4

Point A: Section failure because of just axial compression (M= 0)

Point B: Section failure because of just one bending moment (N = 0). The neutral axis is placed in such a way that there is internal forces balance in the section.

Point C: Its abscissa is the same as point B ($M_{pl.Rd}$). Failure axial force ($N_{pl.Rd}$) equals the bearing capacity both for concrete under compression and steel placed within the central region with a height of $2 \cdot h_n$.

Point D: Neutral axis is placed on the whole section center of gravity. Failure bending moment ($M_{\max,Rd}$) is determined with the plastic section modulus of concrete, structural steel and rebars.

Fig. 1(b) depicts all the plastic stresses blocks for any of the four representative points used for the interaction diagram tracing of a concrete encased structural steel section according to its strong axis.

In the case of short columns it is enough to check that the point defined by the pair of values N_d and M_d is placed within the area that the interaction diagram encloses (Kwak and Kwak 2010).

Checking slender columns affected by second order effects according to this method consists of verifying that the bending moment value M_d doesn't go beyond the bending bearing capacity affected by coefficient μ_d (see Fig. 2). This ratio takes into account the element slenderness and its buckling mode. It is obtained from the same interaction diagram as long as it is represented in a non-dimensional manner.

A non-linear analysis provides a smaller strength value than the one obtained by means for the method because the structural steel and reinforcing steel is not fully exploited (due to the strain of the concrete in compression is limited) (Valach and Gramblicka 2007).

Thus, a correct section interaction diagram tracing has an extremely important role when designing concrete encased columns.

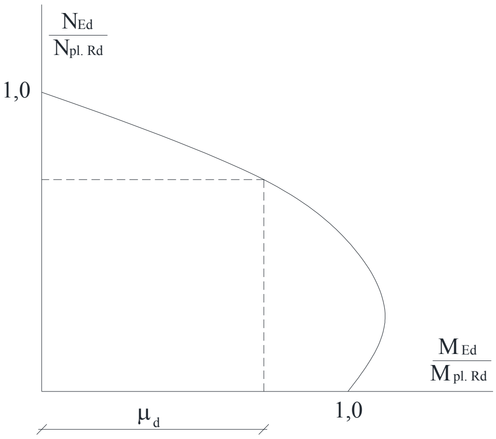

Fig. 2 Interaction diagram for columns design

3. Strain compatibility method

An alternative analysis to that one considering pure plastic behavior can be suggested departing from the hereunder basic hypothesis:

- Plain sections remain plain after the deformation (Navier Hypothesis). Strains vary proportionally to their distance to the neutral axis. Stress on each point is obtained from its strain taking into account the materials nonlinear constitutive laws.
- Section failure will happen when failure strain is reached at any of the materials that it is made of.
- There is deformational compatibility between steel and concrete in their contact surfaces.
- Computations included in this article consider the ensuing stress-strain relationships for materials:

3.1 Concrete

We will use the concrete behavior idealization proposed by Eurocode 2 (2004) for sections design (Fig. 3(a)). Maxim strain ε_{cu} adopted in this diagram is 0,35%.

Stress-strain relationship can be expressed by these functions

$$\begin{array}{ll} -0{,}002 < \varepsilon_c < 0 & \sigma_c = 1000 \cdot \varepsilon_c \cdot (250 \cdot \varepsilon_c + 1) \cdot f_{ck} \\ -0{,}035 \le \varepsilon_c \le -0{,}002 & \sigma_c = f_{ck} \end{array} \quad (1)$$

3.2 Reinforcement and profile steel

According to Eurocode 4, we will adopt stress-strain simplified curves constituted by two branches (Fig. 3(b)). A first branch departs from the origin and reaches the characteristic yield stress with a gradient which equals *Es* adopting a value of 210 N/mm^2. A second branch with a gradient which equals *Es*/1000, departs from the characteristic yield stress and reaches the maximum strain with a value of 1%.

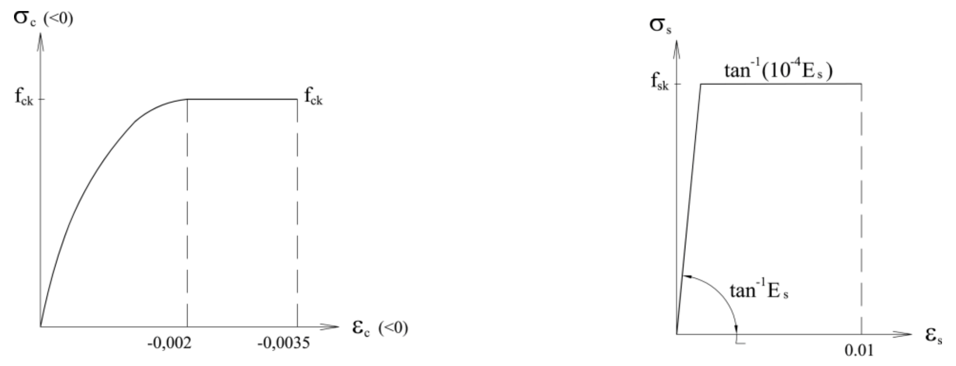

(a) Concrete (b) Steel

Fig. 3 Strain-stress diagrams

3.3 Elastic-plastic stresses distribution all over the section

Applying the so named design hypotheses and the materials stress-strain relationships consideration, we will obtain several stress diagrams all over the section depending on the neutral axis position.

As an example Fig. 4 depicts the strain failure plane and the corresponding stress diagrams because of just one bending moment (point B of the interaction diagram according to Eurocode 4 method). The neutral axis position produces the section forces equilibrium.

Readers can observe that the depicted steel profile is not completely yielded as long as even one of the flanges is under elastic behaviour. Elastic zone extension will depend on the materials strengths and the relationship between the profile depth and the concrete section depth.

Differences with those diagrams with rectangular stresses blocks as employed by Eurocode 4 method (Fig. 1(b)) are obvious. When neutral axis cuts the steel profile (points B, C and D according to Eurocode 4) a portion of the profile is not yielded and the concrete compressive block area which is closer to the neutral axis is under a smaller stress than the concrete's strength.

Using a plastic model or an elastic-plastic one for the materials leads to different failure forces for the section. These differences are more or less important depending on the neutral axis position.

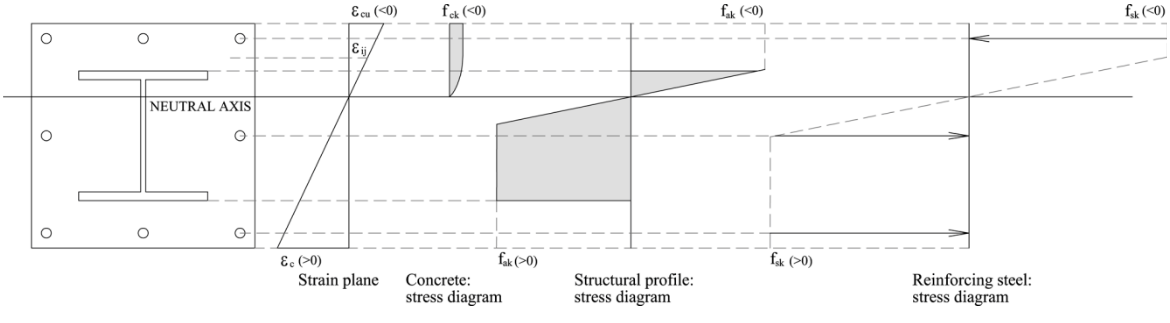

Fig. 4 Strain and stress distribution on the section

3.4 Section analysis procedure

Using an elastic-plastic model with nonlinear constitutive laws for materials requires integrating stresses on the whole section in order to determine failure forces. In this case this integration has been carried out by means of software (Fenollosa and Cabrera 2013) which uses a fiber model (Dundar *et al*. 2008, Polatov 2013).

When compression axial force and one bending moment occurs the process begins placing the neutral axis position which is defined by its distance to the center of mass (z_n) and imposing the section failure condition. With a known failure plane curvature ($\phi = \varepsilon_{cu} / z$), we will obtain strain of each fiber by multiplying the curvature by its distance to the neutral axis ($\varepsilon_i = \phi \cdot f_i$).

Each fiber stress is obtained by applying the non-linear constitutive equation of the material which it is made of. Internal forces produced by the initial configuration (z_n - ϕ) corresponding to certain section failure values (N_u, M_u) will be obtained by applying the hereunder expressions

$$N_u = \sum_i \sigma_i \cdot A_i \tag{2}$$

$$M_{Yu} = \sum_i \sigma_i \cdot A_i \cdot z_i \tag{3}$$

Main differences between this previous process for obtaining the points which define the interaction diagram and the Eurocode 4 process consist of two aspects:

- As long as it is a computer assisted process it is possible to obtain as many points of the diagram as desired just by determining a new position for the neutral axis.
- We will not consider stresses for each point constant and with the value of each material design strength. Their value will be obtained from the constitutive equation which relates stress and strain for each material.

3.5 Interaction diagrams comparison

In order to verify the incidence of the use of a plastic model or an elastic-plastic one for the materials interaction diagrams for several concrete encased sections have been elaborated following both procedures previously described.

Usual 35x35cm section with 4ϕ20 as reinforcement bars placed with a 3 cm depth coating will be considered. The process verifies incidence of the steel profile by using three different sizes: HEB-120 (Fig. 5(a)), HEB-180 (Fig. 5(b)) and HEB-240 (Fig. 5(c)). I also quantifies concrete strength effect by using two different types of concrete with f_{ck} = 25 MPa and f_{ck} = 40 MPa, respectively.

Anyway structural steel strength will be f_{yk} = 275 MPa and rebars steel strength will be f_{sk} = 400 MPa. Partial safety coefficients adopted will be γ_c = 1,5, γ_s = 1,15 and γ_y = 1,10.

As it can be observed in Fig. 5 diagrams Plastic Stress Distribution Method (P.S.D.M.) and Strain Compatibility Method (S.C.M.) provide identical results for the just compression axial force failure point (A) and sufficiently close results for just one bending moment failure point (B). Differences become noticeable when analyzing the maximum bending moment which the section can bear, getting closer when the axial force becomes more important than the bending moment (intermediate zone between points A and C).

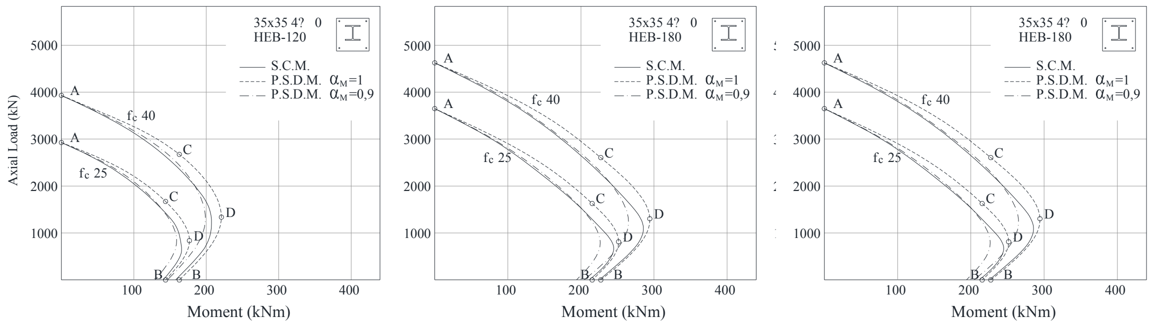

(a) HEB-120 (b) HEB-180 (c) HEB-240

Fig. 5 Interaction diagram comparative

In this referred stretch, results provided by the method used by Eurocode 4 overvalue the section bearing capacity. Maximum difference is produced in the nearby of point C reaching a maximum value of 8%. Differences are similar in the different analyzed cases. Therefore influence of the relationship between the section and the structural profile sizes and of the concrete strength are not to be considered relevant.

Because of the overvaluation produced when this method is employed, article 6.7.3.6 of the Eurocode weights flexural strength by applying the coefficient α_M when verifying the column bearing capacity (Eq. (4)).

$$\frac{M_{Ed}}{\mu_d \cdot M_{pl,Rd}} \leq \alpha_M \tag{4}$$

Being μ_d the coefficient for axial force and bending moment design defined in Fig. 2. α_M coefficient results 0,9 for steels whose types are between S235 and 355, and results 0,8 for steels whose types are S420 or S460. The impact of α_M is beyond dispute when observing the corresponding interaction diagrams in Fig. 5.

4. Adapted formulation for an elastic-plastic model

It is possible to introduce some simple modifications to the Eurocode 4 method in order to make the obtained interaction diagrams more similar to those results of applying the Strain Compatibility Method.

4.1 Concrete compressive stresses characterization

Stresses in the concrete compressive area can be characterized by the so named Whitney stress block (Whitney and Cohen 1956) where a concrete constant stress with a value of $\eta \cdot f_{cd}$ is assigned to a height of $\lambda \cdot x$ being:

η is a coefficient which corrects design strength adopting a value of 1,0 for concrete strengths not bigger than 50 MPa.

λ is a coefficient which corrects the concrete compressive block in order to take into account the non-linear relationship between stress and strain (Aschheim *et al*. 2007). It adopts a value of

0,8 for concrete strengths not bigger than 50 MPa.

4.2 Structural profile stresses characterization

As long as the structural profile is not completely yielded, an elastic-plastic model will be applied by quantifying in a different way the area under elastic behavior according to the neutral axis position.

Departing from the so exposed criteria Fig. 6 represents the stresses diagrams for five neutral axis characteristic positions. As a result of obtaining the resultant force and the resultant moment produced by these stresses five pairs of values N_u and M_u can be obtained and employed for the section interaction diagram tracing.

5. Proposed elastic-plastic formulation

Next equations characterizing the five representative points will be developed according to the elastic-plastic model application:

5.1 Point a

It corresponds to the section failure under just compression axial (M=0). There is concordance between both explained methods. Therefore section strength for compression Na can be obtained by adding up the yield strength of each of its components (Fig. 6(a)).

$$N_a = \left(A_c \cdot 0{,}85 \cdot f_{cd}\right) + \left(A_a \cdot f_{yd}\right) + \left(A_s \cdot f_{sd}\right) \tag{5}$$

5.2 Point b: $z_n = -(h - t_f)/2$ *respect the center of mass*

This point is obtained when placing the neutral axis on the midline of the upper profile flange: $z_n = -(h - t_f)/2$. Because of this flange reduced stresses their contribution can be disregarded when assessing forces. The upper half of the web will be considered under elastic behavior and the rest of the profile and the rebars will be considered yielded (Fig. 6(b)).

Axial force and bending moment failure for the sections will be obtained as the summation of the concrete, structural profile and rebars contributions.

For this point and next to come the compressed block height and their lever arm with respect to the section axis can be obtained with the hereunder expressions

$$A_c = b_c \cdot 0{,}8 \cdot \left(\frac{h_c}{2} + z_n\right) \tag{6}$$

$$z = \frac{h_c}{2} - 0{,}8 \cdot \left(\frac{h_c}{4} + \frac{z_n}{2}\right) \tag{7}$$

Note that in point B the neutral axis position is to be considered negative.

Expressions for the failure axial force will be

$$N_b = N_{b,c} + N_{b,a} + N_{b,s} \tag{8}$$

$$N_{b,c} = 0{,}85 \cdot f_{cd} \cdot \left(A_c - \frac{b \cdot t_f}{2} - \sum_{i=1}^{n} A_{c,si} \right) \tag{9}$$

$$N_{b,a} = f_{yd} \cdot \frac{A_a}{2} + \frac{1}{2} \cdot f_{yd} \cdot t_w \cdot \left(\frac{h - 2 \cdot t_f}{2} \right) \tag{10}$$

$$N_{b,s} = \sum_{i=1}^{n} f_{sd} \cdot A_{si} \tag{11}$$

Expressions for the failure bending moment will be

$$M_b = M_{b,c} + M_{b,a} + M_{b,s} \tag{12}$$

$$M_{b,c} = 0{,}85 \cdot f_{cd} \cdot \left[(A_c \cdot z) - \left(\sum_{i=1}^{n} (A_{c,si} \cdot e_i) \right) \right] \tag{13}$$

$$M_{b,a} = f_{yd} \cdot \frac{A_a}{2} \cdot z_{g,a} - \frac{1}{2} \cdot f_{yd} \cdot t_w \cdot \frac{(h - 2 \cdot t_f)^2}{12} \tag{14}$$

$$M_{b,s} = \sum_{i=1}^{n} f_{sd} \cdot A_{si} \cdot e_i \tag{15}$$

These expressions require the design strength value introduction respecting the right sign. Resultant axial force can be compression or tension depending on the elements dimensions and the materials strengths.

5.3 Point c: Means $z_n = 0$ in relation to the center of mass

It corresponds to a point obtained by placing the neutral axis on the section symmetry axis (Fig. 6(c)).

Axial force N_c is that one provided by compressed concrete as long as parts under tension and compression of the rest of the components of the section are balanced

$$N_c = 0{,}85 \cdot f_{cd} \cdot \left(A_c - \frac{A_a}{2} - \sum_{i=1}^{n} A_{c,si} \right) \tag{16}$$

The section failure bending moment M_c can be obtained with the summation of the moments produced by concrete, structural profile and rebars. Compressed concrete contribution $M_{c,c}$ can be determined by multiplying the concrete compressive area by its lever arm. We have taken away the effects of the profile and rebars compressive area as long as their contribution will be assessed afterwards.

$$M_{c,c} = 0{,}85 \cdot f_{cd} \cdot \left[(A_c \cdot z) - \left(\frac{A_a}{2} \cdot z_{g,a} \right) - \left(\sum_{i=1}^{n} (A_{c,si} \cdot e_i) \right) \right] \tag{17}$$

Structural profile contribution $M_{c,a}$ has to be assessed in a different way depending on its size with respect of the concrete section height. If $h > 0{,}4h_c + t_f$ then profile flanges are yielded and the web is under elastic behavior.

$$M_{c,a} = \left(W_{pl,f} + W_{el,w}\right) \cdot f_{yd} \tag{18}$$

If $h<0{,}4h_c\ t_f$ then the whole profile is still under elastic behavior

$$M_{c,a} = W_{el} \cdot f_{yd} \tag{19}$$

Rebars contribution $M_{c,s}$ will be assessed considering them yielded

$$M_{c,s} = \sum_{i=1}^{n} f_{sd} \cdot A_{si} \cdot e_i \tag{20}$$

5.4 Point d. Means $z_n = (h - t_f) / 2$ in relation to the center of mass

It corresponds to a point as a result of placing the neutral axis in the intermediate line of the profile inferior flange $z_n = (h - t_f)/2$. Because of the small stresses in that flange their contribution when assessing the forces will be disregarded.

Failure axial force and bending moment for the section N_d will be obtained as the summation of concrete, structural profile and rebars contributions.

When assessing the structural profile contribution the effects of the flange crossed by the neutral axis will be disregarded, one half of the web will be considered under elastic behavior and the rest of the profile and the rebars will be considered yielded (Fig. 6(d)).

Applying these criteria we will obtain the failure axial force

$$N_d = N_{d,c} + N_{d,a} + N_{d,s} \tag{21}$$

$$N_{d,c} = 0{,}85 \cdot f_{cd} \cdot \left(A_c - A_a - \sum_{i=1}^{n} A_{c,si} \right) \tag{22}$$

$$N_{d,a} = f_{yd} \cdot \frac{A_a}{2} + \frac{1}{2} \cdot f_{yd} \cdot t_w \cdot \left(\frac{h - 2 \cdot t_f}{2} \right) \tag{23}$$

$$N_{d,s} = \sum_{i=1}^{n} f_{sd} \cdot A_{si} \tag{24}$$

Failure bending moment value will be obtained with the ensuing equations

$$M_d = M_{d,c} + M_{d,a} + M_{d,s} \tag{25}$$

$$M_{d,c} = 0{,}85 \cdot f_{cd} \cdot \left[\left(A_c \cdot z\right) - \left(\frac{A_a}{2} \cdot z_{g,a} + t_w \cdot \frac{z_n^2}{2} \right) - \left(\sum_{i=1}^{n} \left(A_{c,si} \cdot e_i\right) \right) \right] \tag{26}$$

$$M_{d,a} = f_{yd} \cdot \frac{A_a}{2} \cdot z_{g,a} - \frac{1}{2} \cdot f_{yd} \cdot t_w \cdot \frac{(h - 2 \cdot t_f)^2}{12} \tag{27}$$

$$M_{d,s} = \sum_{i=1}^{n} f_{sd} \cdot A_{si} \cdot e_i \tag{28}$$

5.5 Point e: Means $z_n = (h - 2 \cdot t_f)/4$ in relation to the center of mass

If the profile and the whole section heights verify $h > 0{,}4h_c + t_f$, then point d moves away excessively from point c (Fig. 7(c)). In order to get more accuracy for the tracing it could be advisable to obtain another interaction diagram point by imposing the neutral axis to be placed at the fourth part of the structural profile web height: $z_n = (h - 2t_f)/4$. On this position and because of the profile size both flanges and half of the web can still be considered yielded and the other half of the web will be considered under elastic behavior. All rebars will be considered then yielded (Fig. 6(e)).

Failure axial force for the section is obtained as the summation of the concrete, structural profile and rebars contribution according to the hereunder expressions

$$N_e = N_{e,c} + N_{e,a} + N_{e,s} \tag{29}$$

$$N_{e,c} = 0{,}85 \cdot f_{cd} \cdot \left(A_c - \left(\frac{A_a}{2} + t_w \cdot z_n \right) - \sum_{i=1}^{n} A_{c,si} \right) \tag{30}$$

$$N_{e,a} = f_{yd} \cdot t_w \cdot \left(\frac{h - 2 \cdot t_f}{2} \right) \tag{31}$$

$$N_{e,s} = \sum_{i=1}^{n} f_{sd} \cdot A_{si} \tag{32}$$

We will obtain the section failure bending moment with the equation

$$M_e = M_{e,c} + M_{e,a} + M_{e,s} \tag{33}$$

$$M_{e,c} = 0{,}85 \cdot f_{cd} \cdot \left[(A_c \cdot z) - \left(\frac{A_a}{2} \cdot z_{g,a} + t_w \cdot \frac{z_n^2}{2} \right) - \left(\sum_{i=1}^{n} (A_{c,si} \cdot e_i) \right) \right] \tag{34}$$

$$M_{e,a} = f_{yd} \cdot \left(\frac{A_a}{2} \cdot z_{g,a} + b \cdot t_f \cdot \frac{(h - t_f)}{2} + t_w \cdot \frac{11 \cdot (h - 2 \cdot t_f)^2}{96} \right) \tag{35}$$

$$M_{e,s} = \sum_{i=1}^{n} f_{sd} \cdot A_{si} \cdot e_i \tag{36}$$

$M_{e,a}$ is the bending moment produced by the compressive half of profile web and its tensile

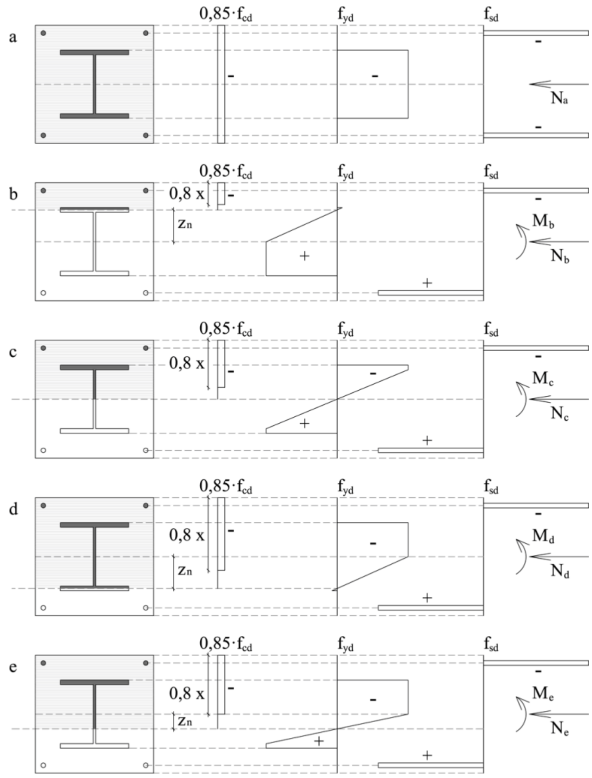

Fig. 6 Stresses diagram. Elastic-plastic model

flange considering both yielded plus the bending moment produced by the tensile forth of the profile web considered under elastic behavior. The contribution of the compressive forth of the profile web under elastic behavior has been disregarded.

6. Proposed formulation application

The proposed formulation verification has been carried out assessing the failure forces for the so described failure points and their superposition with those diagrams result of applying the Strain Compatibility Method (see Fig. 7).

As an example of the developed checks Fig. 5 interaction diagrams are presented again now displaying those points obtained by means of the elastic-plastic formulation.

A total correspondence for point a (centered axial force) can be observed on the interaction diagrams. As for the other points deviations are always negligible and depend on the particular characteristics of each section.

Point c is obtained when placing the neutral axis on the section axis and leads to a position which is close to the maximum bending moment that the section can bear.

Point b depends on the section characteristics and can be placed either in the nearby of the pure bending with no axial force (Fig. 7(a)) or can be places in such a way that the failure axial force is a tensile one (Figs. 7(b)-(c)).

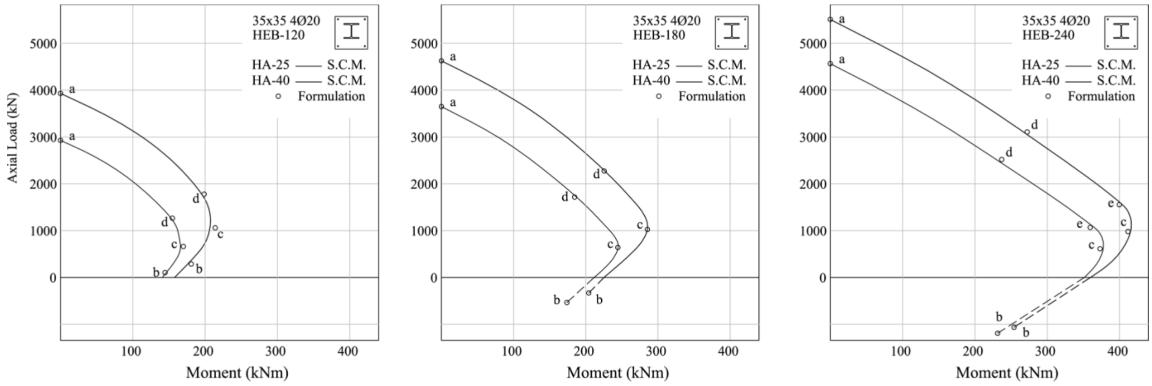

(a) HEB-120 (b) HEB-180 (c) HEB-240

Fig. 7 Proposed formulation verification

7. Conclusions

Interaction diagram for a composite section under axial force and a single bending moment can be obtained either departing from a plastic stress distribution (EC4 2011) or by integrating the section stresses according to the strain compatibility criteria.

The use of stress rectangular blocks inherent to the plastic stress distribution method overvalues the section bearing capacity, especially when the compression axial force comes with high bending moment values. Thus Eurocode 4 weights these bending moment values with the α_M correction coefficient prior to the curves tracing.

Strain Compatibility Method should be used when more precision is demanded and no weighting is desired. But it involves a huge complexity for the stresses integration so computer-assisted procedures are usually required.

Preserving the same criteria of an elastic-plastic stress distribution, this paper has presented alternative and simplified expressions for concrete encased sections which enable practitioners to determine the failure internal forces in five significant points of the interaction diagram having considered five different positions of the neutral axis. These expressions are simple enough to be used as an alternative procedure to the computer assisted stresses integration, as long as a sufficiently concordant interaction diagram can be traced relying strictly on these five points.

Finally, in order to demonstrate the reliability of the proposed expressions, several examples have been given. Interaction diagrams for three different concreted encased sections considering two different concrete strengths have been represented as a result of a computer assisted strain compatibility method application. Failure internal forces for the abovementioned five points have been placed on these diagrams revealing a very good correspondence with them and with the Eurocode weighted curves as well. Thus it has been verified that this formulation is valid not only for different structural profile sizes but also for different concrete strengths.

References

AISC (2005), Load and resistance factor design specification for structural steel buildings, American Institute of Steel Construction; Chicago, IL, USA.

Aschheim, M., Hernández-Montes, E. and Gil-Martín, L.M. (2007), “Optimal domains for strength design of rectangular sections for axial load and moment according to Eurocode 2", *Eng. Struct.*, **29**(8), 1752-1760.

BS 5400 (2005), Steel, concrete and composite bridges: Part 5: Code of practice for design of composite bridges, British Standards Institution; London, UK.

Dundar, C., Tokgoz, S., Tanrikulu, A.K. and Baran, T. (2008), "Behavior of reinforced and concrete-encased composite columns subjected to biaxial bending and axial load", *Build. Environ.*, **43**(6), 1109-1120.

Ellobody, E. and Young, B. (2011), "Numerical simulation of concrete encased steel composite columns", *J. Constr. Steel Res.*, **67**(2), 211-222.

Ellobody, E., Young, B. and Lam, D. (2011), "Eccentrically loaded concrete encased steel composite columns", *Thin. Wall. Struct.*, **49**(1), 53-65.

Eurocode 2, EC2 (2004), Design of concrete structures. Part 1-1: General rules and rules for building, European Committee for Standardization; Brussels, Belgium.

Eurocode 4, EC4 (2011), Design of composite steel and concrete structures. Part 1-1: General rules and rules for building, European Committee for Standardization; Brussels, Belgium.

Fenollosa, E and Cabrera, I. (2013), "Analysis of composite section columns under axial compression and biaxial bending moments", In: *Structures and Architecture: Concepts, Applications and Challenges*; (Chapter 186), Taylor & Francis Group, London, UK. pp. 1498-1505.

Griffis, L.G., Moore, W.P. and Associates, Inc. (2003), Steel design guide series 6. Load and resistance factor design of W-shapes encased in concrete, American Institute of Steel Construction.

Johnson, R.P. (2004), C*omposite Structures of Steel and Concrete*, Volume 1: Beams, Columns, Frames and Applications in Building, (3th Edition), Blackwell Publishing, Oxford, UK.

Jung, I.K., Shim, C.S., Chung, Y.S., Min, J. (2005), "Experiments for the evaluation of P-M interaction curve of SRC composite columns", *J. Kor. Soc. Civil Eng. Magazine*, **25**(3A), 555-563

Kwak, H. and Kwak, J. (2010), "An improved design formula for biaxially loaded slender RC column", *Eng. Struct.*, **32**(1), 226-237.

Polatov, A. (2013), "Numerical simulation of elastic-plastic stress concentration in fibrous composites", *Coupled Syst. Mech., Int. J.*, **2**(3), 271-288

Roik, K. and Bergmann, R. (1989), Eurocode 4: Composite columns. Report EC4/6/89; University of Bochum, Bochum, Germany.

Saw, H.S. and Richard Liew, J.Y. (2000), "Assessment of current methods for the design of composite columns in buildings", *J. Constr. Steel Res.*, **53**(2), 121-147.

Shanmugam, N.E. and Lakshmi, B. (2001), "State of the art report on steel-concrete composite columns", *J. Constr. Steel Res.*, **57**(10), 1041-1080.

Soliman, K.Z., Arafa, A.I, and Elrakib, T.M. (2013), "Review of design codes of concrete encased steel short columns under axial compression", *Housing Building National Research Center*, **9**(2), 134-143.

Tokgoz, S. and Dundar, C. (2008), "Experimental tests on biaxially loaded concrete-encased composite columns", *Steel Compos. Struct., Int. J.*, **8**(5), 423-438.

Valach, P. and Gramblicka, S. (2007), "Theoretical and experimental analyses of composite steel-reinforced concrete (SRC) columns", *Slovak J. Civil Eng.*, **1**(4), 1-9.

Whitney, C.S. and Cohen, E. (1956), "Guide for ultimate strength design of reinforced concrete", *ACI J.*, **28**(5), 445-490. [Proceedings V.53]

CC

Nomenclature

We have used the following symbols in this paper

A_a	Area of the structural profile section
A_c	Area of compressed concrete
$A_{c,si}$	Area of each of the rebars placed in the compressed zon
A_i	Area of each one of the fibers
A_{si}	Area of each of the rebars
b	Width of the structural profile
b_c	Width of the concrete section
f_{ck}	Characteristic strength for concrete
f_{cd}	Design strength for concrete
f_{sk}	Characteristic strength for reinforcement steel
f_{sd}	Design strength for reinforcement steel
f_{yk}	Characteristic strength for the structural profile steel
f_{yd}	Design strength for the structural profile steel
h	Depth of the structural profile
h_c	Depth of the concrete section
M_{Ed}	Bending moment design value
$M_{pl,Rd}$	Composite section plastic bending moment capacity design value
$M_{a,a}$	Contribution of the structural profile steel to the bending moment in point “a”. If any other point is considered just switch “a” by the new point name
$M_{a,c}$	Contribution of concrete to the bending moment in point “a”. If any other point is considered just switch “a” by the new point name
$M_{a,s}$	Contribution of rebars to the bending moment in point “a”. If any other point is considered just switch “a” by the new point name
M_{Yu}	Ultimate bending moment about Y for the section
M_{Zu}	Ultimate bending moment about Z for the section
$N_{a,a}$	Contribution of the structural profile steel to the axial force in point “a”. If any other point is considered just switch “a” by the new point name
$N_{a,c}$	Contribution of concrete to the axial force in point “a”. If any other point is considered just switch “a” by the new point name
$N_{a,s}$	Contribution of rebars to the axial force in point “a”. If any other point is considered just switch “a” by the new point name
N_u	Ultimate axial force for the section
t_f	Flange thicknesses of the structural profile

t_w	Web thicknesses of the structural profile
x	Compressed zone depth measured from the neutral axis to the section edge
y_i	Distance from each cell center of gravity to reference axis Z of the section
z	Lever arm of the compressed block referred to section axis
z_i	Distance from each cell center of gravity to reference axis Y of the section
z_n	Depth of the neutral axis to the reference axis of the section
z_g	Center of mass of half structural profile in relation to the whole section center of mass
α	Fatigue coefficient for concrete
α_M	Axial and bending moment design coefficient for columns
γ_c	Partial factors of safety for concrete
γ_s	Partial factors of safety for reinforcement steel
γ_y	Partial factors of safety for the structural profile steel
ε_c	Concrete strain
ε_{cu}	Failure concrete strain
λ	Correcting factor for compression block concrete depth
μ_d	Correcting factor for composite section bending moment capacity when designing columns
η	Correcting factor for concrete design strength
σ_c	Concrete stress
σ_i	Design stress at each fiber